A NEW SYMMETRICAL FAR INFRARED NEBULA AT -33^{O} DECLINATION

B. Aryal*, **K. Simkhada***, **C. Rajbahak*** & **R. Weinberger****
*Central Department of Physics, Tribhuvan University, Kirtipur, Kathmandu, Nepal.
**Institute of Astroparticle Physics, Innsbruck University, Innsbruck, Austria.

Abstract: A systematic search at far infrared wavelength in IRAS (Infrared Astronomical Satellite) survey using Groningen Server is performed and investigated a new symmetrical far-infrared (~3^{o} x 2^{o}) filamentary emission at R.A. (J2000) = 21^{h}28^{m}51^{s} and Dec. (J2000) = -33^{o}53'23''. The softwares ALADIN2.5 and ASTROLINUX5.0 are used for the data reduction. We have performed multiwavelength study in the region of interest. The physical properties, flux density, temperature and mass of the nebula are estimated and discussed. In the multiwavelength study, the optical and ultraviolet emission is found to be negligible. A significant far infrared emission is noticed. The radio and X-ray emission is observed to be moderate. It is found that there is a maxima in each filaments, that can clearly seen in 60 μm and 100 μm wavelengths. This indicates that the structure is nearby and a strong external force is influencing its shape. No star is forming in our region of interest. Our symmetrical far infrared nebula belongs to category II type cloud, appearing as diffuse emission of nearly faint optical surface brightness but showing a clumpy structure with no star forming. Total mass of the gas of our nebula is found to lie in the range 1.275 – 3.000 x 10^{3} M_{sun}. This estimation is based on the results of flux density study assuming a distance 150±50 pc and dust color temperature 25±5 K.

Key Words: Interstellar Medium; Stars; Nebula; Infrared Emission.

PROBLEM IDENTIFICATION

The IRAS all-sky maps turned out to be useful in many respects, e.g. by demonstrating that dust structures are ubiquitous and come in all kinds of shapes and sizes. Although the IRAS mission took place two decades ago - the maps are still not exhausted of their riches, as we could demonstrate very recently by the discovery of the first jets (size ~ 9^{o} each) found in the far infrared (Weinberger & Armsdorfer 2004) and first pulsar pumped nebula (Aryal & Weinberger 2006). It is interesting to search new filamentary structures in the IRAS survey. We have carried out all sky survey covering galactic latitude between 0^{o} to -90^{o}. This region is less studied. We expect to find new filamentary structures as investigated by Odenwald & Rickard (1987). It is believed that the shaping of infrared dust structure has a close relation with the inhomogeneous Interstellar Medium (ISM). The violent stellar phenomena lead inhomogeneity in the ISM. We are interested to perform multiwavelength study in the emission region. This may reveal the importance of hot gas (X-rays, UVs, etc) in the shaping process.

The search of the nebula responsible for the infrared emission remains a challenging task in Infrared Astronomy. The question of chance superposition is becoming a vital issue. Unfortunately there is no convincing way to find out this, since a lot of structure in the IRAS maps exists at all scales, and particularly there is a multitude of variously shaped clouds, blobs, arcs, filaments, holes, etc. Nevertheless, we intend to carry out a study to address this problem of superposition on IRAS maps. It would be interesting to search for any (stellar) objects which might be capable of shaping an interstellar cloud of small or moderate mass; such an object should be located at or around the extended emission (Aryal & Weinberger 2002, 2003, 2004, 2006). With SIMBAD, we intend to investigate discrete sources in the field of the infrared emission (if any) that might be responsible in the shaping of IR-cloud. We use the method developed by Henning et al. (1990) and Hildebrand (1983) in order to estimate the mass of the dust and the gas of the IR-cloud (ROI) using ALADIN 2.5 and FITSVIEW 2.0.1 software.

SYSTEMETIC SEARCH IN THE IRAS MAP

A systematic search in the IRAS maps is performed during October 2005 to March 2006. This was done in following six steps:

Author for Correspondence: B. Aryal, Central Department of Physics, Tribhuvan University, Kirtipur, Kathmandu, Nepal.

(1) Inspection of the region in 3^o x 3^o in IRAS server which is at the Groningen, The Netherland. As a collaborator, we were able to connect their server via internet (http://www.skyview@skyview.gsfc.nasa.gov): The input parameters used for the search are as follows: Co-ordinate: Equatorial; Projection: Gnomonic; Image Size: 500 x 500; Brightness Scaling: Histogram Equilization; Equinox: 2000; Pixel re-sampling: Nearest neighbour

(2) Re-examination of the region observed in step 1: Each region is cross checked for overlapping region. For this we inspected the region in 2.5^o x 2.5^o and 7.5^o x 7.5^o. The input parameters remained the same as in step 1. Any emission of size (major diameter) $>0.5^o$ is selected. We selected 84 such regions as a first sampling.

(3) Download the FITS image of the selected region: We selected FITS format of the image for the data processing. The FITS image carries the information concerning the flux density of each pixel. The size of the downloaded images was ~900 MB.

(4) Measurement of the size of the emission using ASTROLINUX2.5 software: At first, the downloaded FITS images were processed in ASTROLINUX2.5 software in order to study the photometric gradient along the major diameters. There are 9 candidates having major diameter > 3^o. ALADIN2.5 software was used to study the contour map of each image. The Re-examination of the arms in these two softwares resulted the rejection of more than 20% of the objects.

(5) Estimate the flux density ratio between the maxima and minima of the emission using ALADIN2.5 software: The contour map of each candidate was studied using ALADIN2.5 software in order to find out the exact position of the maxima and minima in the emission region.

(6) Final selection of the image: We considered the size and the flux density gradient to select the best region of extended emission. We selected 3^o x 3^o region centered at R.A. (J2000) = $21^h\ 28^m\ 51^s$, Dec. (J2000) = $-33^o\ 53'\ 23''$ as our region of interest. The region of interest is shown in Fig. 1a.

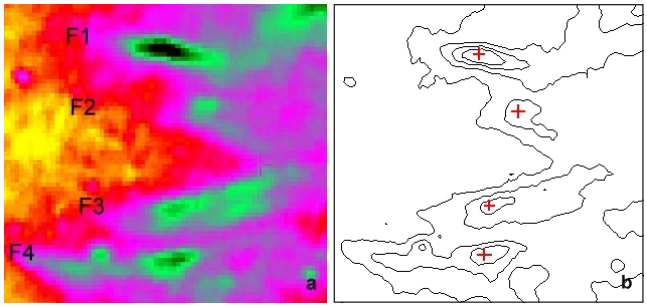

Figure 1: (a) 3^o x 3^o IRAS 100 μm image of our region of interest. Four symmetrical filaments (F_1, F_2, F_3, F_4) can be seen. It seems that the upper two filaments have a close connection with their corresponding lower filaments. The second and third filaments seem to be connected. (b) Contour map of the field as shown in Fig. 3a. This field is centered at R.A. (J2000) = $21^h\ 28^m\ 51^s$, Dec. (J2000) = $-33^o\ 53'\ 23''$. The maxima of the filamentary structures are represented by plus sign.

This structure is rare in the sense that the previous authors (Odenwald 1988, Odenwald & Rickard 1987) discovered a large number of asymmetrical filamentary structures in the IRAS map. Our structure is not yet seen in the literatures till Feb 2009. Another important thing about our symmetrical filaments is the presence of a nearby pulsar around western side of the inner structure. The contour map of our investigated region is shown in Fig. 1b. In the contour map, one can notice that, (1) all four filamentary structures have a maxima, (2) these filaments are loosely connected, (3) a bow shock like effect can be seen in the eastern side, (4) the upper and lower filamentary structures are extended than the inner two structures, (5) the upper structure seem to be connected with huge infrared emission in the western part. Due to its symmetrical appearance and the location, we intend to explore the physical properties of this emission as well as the shaping cause. Our aim is to justify the close association of these four filamentary structures.

RESULTS

1. Categorizing the Emission

Odenwald (1988) carried out optical and far-infrared studies on 14 high Galactic latitude infrared clouds with comet-like or filamentary appearances. He classified these clouds in three catagories named as Catagory I, II and III. Category I clouds is an emission type nebula appearing as dark diffuse appearance of

nearly constant optical surface brightness but showing a disk type internal structure, comprise the objects G64-26, G208-28, G225-66, G228-27, G239-15 as well as the Draco cloud, G90+38. Odenwald (1988) estimates that category II clouds have relatively low dust masses in the range 3-40 M_{sun} and surface brightnesses typical for clouds illuminated by the general interstellar radiation field.

The red-sensitive Dizitized Sky Survey (DSS) image of our region of interest showed no prominent emission. However, a light filamentary trace along north-south direction is seen. No emission can be seen from the filamentary region. Thus, our symmetrical structure belongs to the 'Category II cloud' of Odenwald (1988) classification. The major diameter extends from east to west. The apparent diameter of this structure is about 2^o. Hence, the symmetrical feature of the structure indicates that some internal force is influencing its shape. The source of this force obviously must be located around the nebula. However, the interaction with the interstellar medium can not be denied.

2. True Size of the Object: the Inclination Angle

Inclination angle is the angle between the line of sight and the rotation axis of the large scale structure. This angle gives a clue regarding the intrinsic flatness (i.e., depth – third dimension) of the structure. It is possible that the emission's long axis is in the skyplane. It can be suspected that the investigated structure is inclined by a certain angle with respect to

the plane of the sky. If it is so we estimate the inclination angle by using equation (Holmberg 1946),

$$\cos^2 i = [(b/a)^2 - (0.20)^2]/(1-0.20)^2 \quad (1)$$

where, i = angle between the line of sight and the normal vector of the plane of the emission, a = major axis of the emission passing across the centre, b = minor axis of the emission crossing across the centre. Here the value 0.20 is the intrinsic flatness of the nearby interstellar cloud, as suggested by Kauch (2002). We measured the diameters of our filamentary structure with the help of ALADIN2.5, as follows:

First filament (F_1):

$a = 13.03^o$ and $b = 3.79^o$, i.e., $b/a = 0.29$

Second filament (F_2):

$a = 7.75^o$ and $b = 5.49^o$, i.e., $b/a = 0.70$

Third filament (F_3):

$a = 3.42^o$ and $b = 1.47^o$, i.e., $b/a = 0.43$

Fourth filament (F_4):

$a = 3.48^o$ and $b = 1.19^o$, i.e., $b/a = 0.34$

Substituting these values in equation (1), we calculate the inclination angle to be 78^o, 46^o, 67^o and, 74^o, respectively for the filaments F_1, F_2, F_3 and F_4. The inclination angle of first and fourth filament nicely correlates with each other. The percentage difference between their inclinations is found 2.63±0.23, indicting a close association. If we rotate these two filaments by 14^o from eastern to the western direction, we get the longest structure. At this angle, the maxima of the structure would lie in the plane and any discrete object which is located within the emission in the east-west would lie within the emission, may be in the north-south direction. In such a case the true size of the emission would be less than by a factor of about 2 times apparent size. In contrast to this, the percentage difference between the inclination of filaments F_2 and F_3 is estimated 18.6±1.4, indicting no correlation. If we rotate these two filaments by 20^o from eastern to the western direction, we get the longest structure. However, these filaments are not so long than that of outer filaments.

3. A Test of Star Forming Region

The four filamentary regions might be dense portions of the nebula containing embedded young stars, i.e., the whole object might perhaps be a star forming region. To check this possibility, we have carried out star-count-method in order to compare the stellar density at the location of the nuclei with the stellar densities of the locations outside. In case of star formation, we would expect noticeable dust extinction, i.e. less stars due to the obscuration or dimming of background stars or perhaps a concentration of newly born stars within the place. The counts are done by dividing the objects in the co-ordinate into sixteen grids. For this purpose, the object is searched within 1 degree. The statistics of the star is very poor that's why we re-binned the region into 8 parts by combining first and send bin and so on. SIMBAD clickable map was used to count stars. Within the region of 1 square degree, the field of the maxima of four filaments was downloaded using SIMBAD.

First filament (F_1):

A few stars are found in each grid. We noticed strong isotropy ($P(>\chi^2) = 0.697$) between the observed and expected number of stars in the filament F_1. We set anisotropy if $P(>\chi^2) < 0.050$.

Second filament (F_2):

Average number of stars in each grid is found similar as in first filamentary region. As earlier found, a strong isotropy ($P(>\chi^2) = 0.710$) is noticed between the observed stars and the expected stars in the around the maxima of second filamentary region.

Third filament (F_3):

Average number of stars in each grid is found less than the previous two filamentary regions. As noted earlier, a strong isotropy ($P(>\chi^2) = 0.884$) is noticed between the observed stars and the expected stars in the around the maxima of third filamentary region.

Fourth filament (F_4):

In the fourth filamentary structure region, the chi-square probability ($P(>\chi^2)$) is found less (0.186) than in the previous case. In the second grid, stars are lacking whereas the grid number 8 contain more stars than the expected. It might be due to the presence of a nearby star near fourth filament. That star might be the part of a nearby globular cluster. Thus our investigated region does not show a star forming region.

3. Flux Density Study

The flux density of the given region is studied by using the ALADIN2.5 Software. The region for the maximum flux in all the four projection like structures is determined. The maximum flux in the four projections in the 12 μm, 25 μm, 60 μm and 100 μm are found different.

Table 1: The relative flux density at the maxima of the first (F_1), second (F_2), third (F_3) and fourth (F_4) filaments. These values are in MJy/str.

Surveys (IRAS)	F_1	F_2	F_3	F_4
12 μm	0.4696	0.1297	0.2551	0.1024
25 μm	0.5026	0.3212	0.3807	0.1556
60 μm	1.2235	0.6489	0.7264	0.6890
100 μm	6.4325	2.9004	3.5495	4.3095

A significant maxima is found in all these filamentary structures (Fig. 2a). Absence of nodes and single maxima in all four filaments suggest the close association between the structures. We draw curves along the filaments (Fig. 2b) and studied the variation of relative flux density in each filaments (Fig. 2c,d,e,f). A single but elongated maxima is found in the filaments F_1 and F_3. The maxima is found to be intense in F_1 (Fig. 2g). The filament F_2 is the least intense. The spectral distribution of the maxima of four filamentary structures in four IRAS survey bands (12 μm, 25 μm, 60 μm and 100 μm) is shown in Fig. 2h. Table 1 lists the value of flux density at the maxima of all four filaments in all four IRAS bands. This plot says that the filaments are closely connected. However, at lower wavelengths (12 μm and 25 μm), the correlation is not very strong.

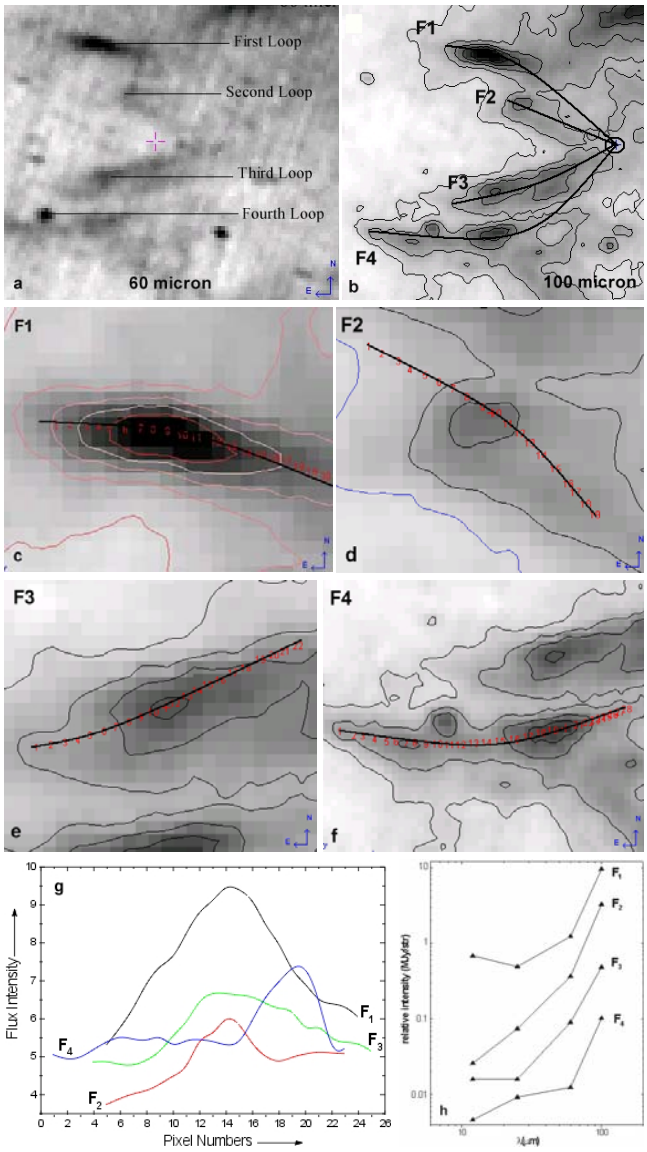

Figure 2: 60 (a) and 100 (b) micron image showing the filaments (or loops). The variation of relative flux density is studied along these filaments (c, d, e & f) separately. (g) A comparison between the relative flux density along the filaments is shown. (h) Spectral distributions of the maxima of four filamentary structures in four IRAS survey bands (12 μm, 25 μm, 60 μm & 100 μm) in the region.

4. Temperature and Distance Estimation

Using the paper by Henning et al. (1990) we have determined the dust color temperature (T_d) of the nebula. The average dust colour temperature in the region was determined to be 27±4 K. We also determined the dust temperature distribution throughout the nebular region by dividing the 100 μm map by the 60 μm map and comparing the resulting F(100 μm)/F(60 μm) values at each map location with the values given for dust grain models by Dwek (1986). We found that the dust color temperature of the filament F_1, F_2, F_3 and F_4 are 29±5 K, 22±4 K, 23±4 K and 31±5 K, respectively. The upper and lower filamentary structures are slightly hotter than the inner filamentary structures. Hence, the locations of the maximum emission i.e., the nuclei of the symmetrical structures are warmer than their filaments.

Our region is at -33 degree declination, the galactic extinction and reddening effect is not significant. This effect is prominent if the declination is less than ±20 degree. Thus we can be precise in assuming the distance because our nebula is far infrared (100 micron) emission type (not the reflection type) (Henning 1990). The maximum physical size of the nebula at this distance then is 8.6 pc, if it lies in the sky plane, and the separation between the upper (F_1) and lower (F_2) filaments is about 3 pc.

5. Mass Estimation

The distance of our region of interest is primarily unknown. In our case, the star count method (Mebold et al. 1985) does not help because of insufficient extinction and too few stars in the region. The nebula also has no obviously embedded stars, which would be helpful for this purpose. Following Odenwald (1988), a distance of 200±50 pc will be assumed for the moment.

As for as the dust color temperature is concerned, it is well known that the IRAS 100 μm wavelength corresponds less than 40 K temperature in any case. By use of the 60 μm and 100 μm fluxes of this region (after subtraction of the background infrared emission) we adopt a dust color temperature of T ~ 25±5 K as an average, using Henning et al. (1990). A temperature of 30 K is only several degrees higher than the interstellar cirrus temperature of ~ 25 K and points to dust heating from the outside, probably from the interstellar radiation field plus a contribution from the inner structure and its source(s) responsible for symmetrical emission. Assuming a gas-to-dust mass ratio of 150 and using a commonly accepted dust mass relation as described in the chapter 3, we estimate total masses of filamentary structures individually. For a comparison, we calculate mass of the gas assuming their respective dust color temperature (29 K for F_1, 22 K for F_2, 23 K for F_3 and 31 K for F_4) (see Table 2).

Table 2: Dust mass estimation for the first (F_1), second (F_2), third (F_3) and fourth (F_4) filaments at their respective dust color temperatures (29 K for F_1, 22 K for F_2, 23 K for F_3 and 31 K for F_4) assuming the distance range 150 pc to 240 pc.

Distance (pc)	M (F_1) in M_{sun}	M (F_2) in M_{sun}	M (F_3) in M_{sun}	M (F_4) in M_{sun}
150	2.72	1.72	1.92	2.14
160	3.14	1.94	2.17	2.42
170	3.41	2.18	2.44	2.71
180	3.94	2.43	2.71	3.02
190	4.32	2.69	3.01	3.35
200	4.77	2.96	3.32	3.70
210	5.24	3.25	3.64	4.06
220	5.73	3.25	3.98	4.43
230	6.26	3.56	4.33	4.83
240	6.71	3.87	4.70	5.24

Thus, the dust mass of the filaments of our symmetrical infrared nebula is found between 1.5 M_{sun} to 20 M_{sun} (distance: 150 to 240 pc and temperature: 20 to 30 K). The first filament is found massive whereas the second is least massive. The esti-

mated dust mass range for first, second, third and fourth are 0.65 M_{sun} to 6.7 M_{sun}, 0.15 M_{sun} to 3.87 M_{sun}, 0.17 M_{sun} to 4.7 M_{sun} and 0.19 M_{sun} to 5.24 M_{sun}, respectively.

As we know that the gas-to-dust ratio is approximately 150 (Aryal & Weinberger 2006). Thus, the total mass of the gas of our investigated nebula lie in the range 1275 M_{sun} (for 150 pc) to 3000 M_{sun} (for 240 pc).

6. Discrete Sources in the Field of the Nebula

In order to find possible candidates for the three successive emissions along a straight line and rounded shape of the emission, we used SIMBAD to locate discrete sources. There are 166 entries within 7 arc minute radius from the first maxima (M1): 78 stars, 29 IRAS sources, 6 nebula, 12 cluster of stars, 1 galactic cluster and 40 others. A list of these sources are given in appendix A. The nearest 5 objects are 2 stars, 1 nebula of unknown nature, 1 infrared source and a molecular cloud. Fig. 3a shows their distribution as well as the position of first maxima.

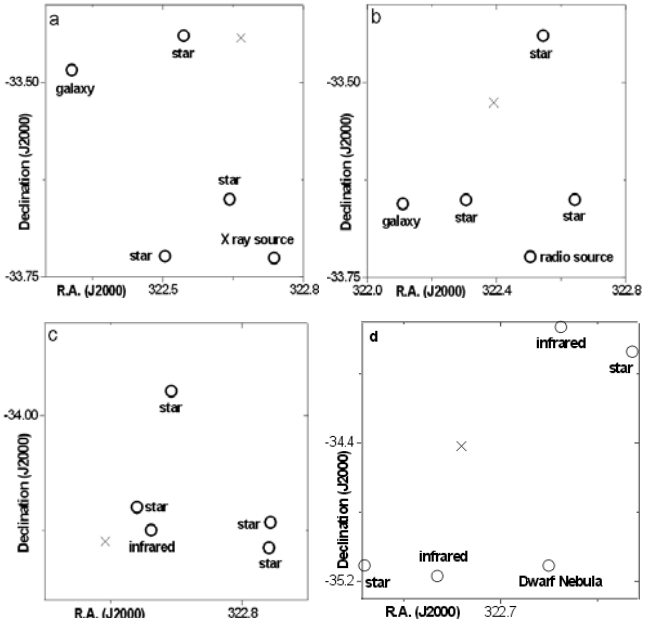

Figure 3: Five nearest neighbor discrete sources around the maxima of the first (upper left, a), second (upper right, b), third (lower left, c) and fourth (lower right, d) filaments. The maxima is represented by a cross mark.

There are 96 entries within 1 square degree around the maxima of first filamentary region (F_1): 42 stars, 11 IRAS sources, 19 galaxies, and 24 others. Five nearest neighbor objects are 3 stars, 1 galaxy, and a X-ray source. Fig. 3a shows their distribution as well as the position around the maxima of the first filament.

There are 92 entries within 1 square degree in the region of maxima in second filamentary region (F_2): 44 stars, 11 IRAS sources, 19 galaxies and 21 others. Five nearest neighbor objects are 3 stars, 1 galaxy, and 1 radio source. Fig. 3b shows their position around the second maxima.

Similarly, the maxima of third filamentary region (F_3) are surrounded by 109 objects within 1 square degree. There are 42 stars, 11 IRAS sources, 23 galaxies and 33 others. Five nearest neighbor objects are 4 stars and 1 infrared source. Fig. 3c shows their distribution around the third maxima.

In the fourth filamentary region (F_4), the total number of objects is 148 within 1 square degree. Among them, 46 stars, 9 IRAS sources, 26 galaxies and 67 others have been observed. Five nearest neighbor objects are 2 stars, 2 infrared source and a dwarf nebula. Fig. 3d shows their distribution around the third maxima.

DISCUSSION

1. Previous Works

A comparison of far-IR spectral distributions of our filamentary structures (F_1, F_2, F_3, F_4) with Draco cloud component (Odenwald & Rickard 1987) is shown in Fig. 4a. The flux density variation from 60 μm to 100 μm is similar in all these plots. This indicates that the dust color temperature profile of our filaments and the Draco cloud component might be similar. In contrast to the Draco cloud component, a slight decrease can be seen when moving from 12 to 25 μm. This type of result is found by Aryal & Weinberger (2006) while studying a Skeleton nebula. Fig. 4b shows a comparison with their work along with MBM 20 (Weiland et al. 1986).

Aryal & Weinberger's (2006) skeleton nebula (first line in Fig. 4b) does not have a strong 12 μm and 25 μm spectral component. This lack of emission at 12 μm and 25 μm suggests that the dust population may be relatively devoid of a small grain component as compared to the cirrus material (Puget et al. 1985), or perhaps that the small dust grain are not being adequately excited by the ambient radiation field (Mebold et al. 1985). The strength of the stellar radiation field near the Draco cloud is estimated to be about 10 times lower than in the Galactic plane (Mebold et al. 1985). The Draco cloud is at 38° latitude, at slightly higher latitude than the skeleton nebula (32°). It is estimated that the stellar radiation field for the skeleton nebula is also weaker (~10-12 times) with respect to a position in the Galactic plane not only because of its high latitude but also due to the smaller number of stars in this region due to the longitude of $l = 197°$.

We have compared results of Aryal & Weinberger (2006), Weiland et al. (1986) and Odenwald & Rickard (1987) by considering their respective estimated mass, size and the position of the emission and found that the stellar radiation field, in our case, is ~8-10 times weaker with respect to a position in the Galactic plane. As for as the temperature is concerned, we rule out that the temperature never pass the limit of 10 K because of the steeper slope from 60 to 100 micron plot. The average slope from 12 to 60 micron is less than the slope from 60 to 100 micron. This indicates that the dust color temperature might lie in between 20 to 30 K. The temperature never cross the 30 K limit if we adopt the result obtained by Odenwald & Rickard (1987) as a correct one.

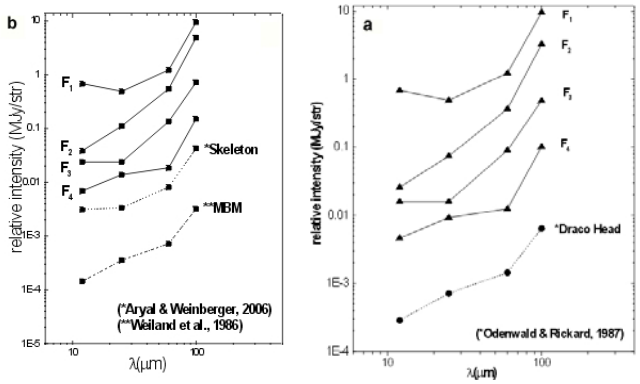

Figure 4: Spectral distributions of the maxima of four filamentary structures in four IRAS survey bands (12 μm, 25 μm, 60 μm & 100 μm) in the region. (a) Comparison with the DRACO cloud component (DRACO-Head) (Odenwald & Rickard 1987) and (b) the Skeleton nebula (Aryal & Weinberger 2006). In this plot, the spectral distribution of the MBM 20 "cirrus cloud" (position no. 1 from table 1, Weiland et al. 1986) is shown. All intensities have been background subtracted and colour corrected for 240 K blackbody emission.

2. Discussion

A multiwavelength comparison of flux emitted from the symmetrical structure is studied. Fig. 5a shows a relative comparison of flux density emitted from our symmetrical far infrared nebula in all investigated wavelengths. In this plot we have added the value of flux density estimated by various surveys for radio, infrared, optical and X-ray region. We noticed that the far infrared emission is dominating without significant emission in optical band. This result suggests that the object is relatively nearby (distance < 500 pc) according to the Odenwald (1988). In addition, a weak emission is noticed from radio and X-rays.

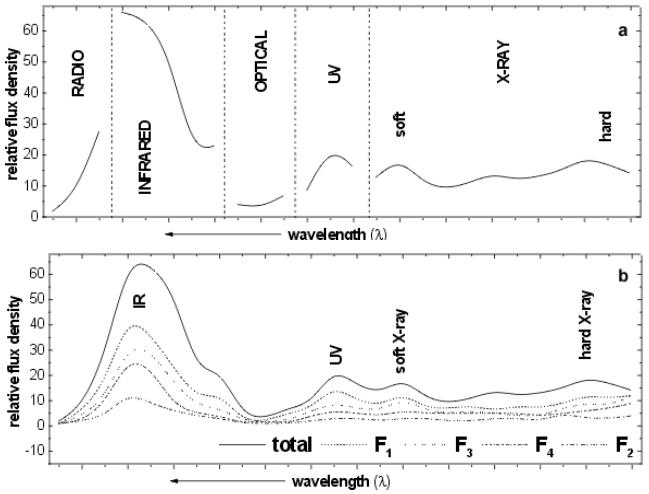

Figure 5: (a) A comparison of relative flux density in various multiwavelengths — radio, infrared, optical, ultraviolet and X-ray wavelengths. (b) A comparison of relative flux density for four filamentary structures (denoted by F_1, F_2, F_3, F_4) in multiwavelength survey.

Radio emission is found increasing with decreasing wavelength (Fig. 5b) as noticed by Mishra (2006). We could not study microwave emission because our region is not yet surveyed for nearby structures in this wavelength. The most interesting region is the infrared. Infrared emission goes on decreasing with increasing frequency. The optical emission is almost negligible. A trace of X-ray (both soft and hard) is noticed. The intensity of soft X-ray emission is relatively higher than the hard X-ray. In Fig. 5b, we suspect that the domination of far infrared flux density is mainly due to the interaction between interstellar medium and the strong stellar wind from the unknown source.

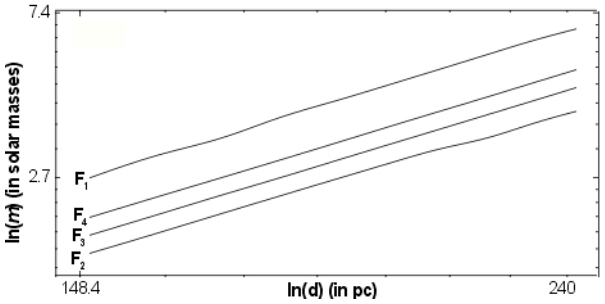

Figure 6: (a) A comparison of estimated mass of the filaments versus the distance in log scales for their respective dust color temperatures. In all temperatures, interestingly, slopes are found to be constant.

As expected, we found that the region is not dominated by the molecular cloud. That's why, we could not notice star forming region in our region of interest.

A comparison of estimated mass (in natural log scale) versus the distance (in natural log scale) is shown in Fig. 6. Interestingly, the slope is found to be constant for all filaments. This result strongly suggests a good correlation between the masses of these four filaments. Thus, the appearance of these structures is not due to the chance superposition. The origin of this structure must have a single cause. That cause might be the strong stellar wind from unknown source or the interaction between the interstellar medium and the relativistic wind emitted from the pulsar (a nearby pulsar is found near second filamentary structure).

CONCLUSION

A systematic search at infrared wavelength in IRAS (Infrared Astronomical Satellite) survey using Groningen IRAS server is carried out.) We investigated a new symmetrical far-infrared (~3° x 2°) filamentary emission at R.A. (J2000) = $21^h28^m51^s$ and Dec. (J2000) = -33°53'23''. The softwares ALADIN2.5 and ASTROLINUX5.0 are used for the data reduction and analysis. We have performed multiwavelength study in the region of interest. In addition, physical property of the object, a test of star forming region, flux density variation, temperature and mass estimation are studied and discussed. We conclude the following:

(1) The investigated symmetrical, filamentary structure is moderate in size (~3° x 2°). Their extension is found to be elongated along east-west direction. There are four filaments, the middle seem to be connected.

(2) The optical and ultraviolet counterpart of the object is found to be weak. Only the infrared counterpart is found strong. The radio and X-ray counterpart is moderate. In other word, our symmetrical object emits photons of infrared, radio and X-ray wavelengths except the ultraviolet and optical. A significant far infrared emission is noticed. This indicates that

the structure is nearby and a strong external force is influencing its shape, might be AGB phase star emitting strong stellar wind or a pulsar emitting relativistic wind. The source of this force obviously must be located outside the nebula.

(3) It is found that there is a maxima in each filament, that can clearly seen in 60 μm and 100 μm infrared wavelength. It seems that the position of these maxima is designed by external agent. However, the association of the inner filaments can not be denied.

(4) The region of interest seems to be passive towards star forming (SFR) around the maxima of all filaments. This is an interesting correlation that the stellar density is extremely low around the maxima of the filaments.

(5) Our object belongs to category II type cloud of Odenwald (1988), appearing as diffuse emission of nearly faint optical surface brightness but showing a clumpy structure with no star forming.

(6) It is found that our emission structure is nearly edge-on type (inclination angle > 45°). The inclination angle of first and fourth filament nicely correlates with each other. In contrast to this, filaments F_2 and F_3 do not correlate with each other. It might be due to the unknown physical connection between them.

(7) There is a rapid decrease of the emission's surface brightness towards longer infrared wavelengths as is evident by comparing the emission at 60 μm and 100 μm, suggesting the moderate temperature (20 to 30 K) for the dust.

(8) In order to find possible candidates for the three successive emissions, we used SIMBAD database to locate discrete sources. There are 96, 92, 109 and 148 entries within 1 square degree radius from the first, second, third and fourth maxima of the filaments, respectively. The presence of a dwarf nebula near fourth maxima is noticeable.

(9) Total mass of the gas of our nebula is found to lie in the range $0.225 – 3.000 \times 10^3 M_{sun}$. This estimation is based on the assumption for the distance as 150±50 pc and dust color temperature as 25±5 K. This suggests that the structure is moderate (not massive). Obviously, it seems true because we suspect that the structure is far infrared nebula.

The shaping mechanism and the cause of the filamentary structure is the main issue that should be addressed in the future. An optical observation the maxima of four filamentary structures are recommended in order to study the cause and nature of the symmetrical far-infrared emission. We discussed this result with Prof Ronald Weinberger, Innsbruck University, Austria. Our joint proposal to observe HII region at 4 maxima of the filamentary emission using 1.8 meter Asiago Observatory, Padua, Italy, is on the pipeline. We expect to get 4 night observation during mid Nov-Dec 2009.

ACKNOWLWDGEMWNTS

We acknowledge Profs. W. Saurer (Innsbruck University, Austria) and U. Khanal (Tribhuvan University, Nepal) for insightful discussions. B. Aryal acknowledges Tribhuvan University, Kathmandu, Nepal for a research leave during Oct-Dec 2007. One of the authors (KS) acknowledges B. P. Koirala Memorial, Planetarium Observatory and Science Museum Development Board, Ministry of Environment, Science & Technology for providing a fellowship to carry out this work.

REFERENCES

[1] Aryal, B. and Weinberger, R. 2006. *Journal Astronomy & Astrophysics*. **366**: 438.

[2] Aryal, B. and Weinberger, R. 2004. Huge Dust Structures and cavities Around PNe: NGC 6826 and NGC 2899. Edited by Margaret Meixner, Joel H. Kastner, Bruce Balick and Noam Soker, *ASP Conf. Proc.*, Vol. **313**. San Francisco: Astronomical Society of the Pacific: 112.

[3] Aryal, B. and Weinberger, R. 2003. Asymmetric mass-loss on the AGB: examples from IRAS data. Edited by Y. Nakada, M. Honma and M. Seki. *Astrophysics and Space Science Library*, Vol. **283**, Dordrecht: Kluwer Academic Publishers, ISBN 1-4020-1162-8: 103.

[4] Aryal, B. and Weinberger, R. 2002. Structure of Interstellar Bubbles: A Numerical Time-Dependent Calculation. Supplementary Issue 2, Vol. **324**, Short *Contributions of the Annual Scientific Meeting of the Astronomische Gesellschaft in Berlin*: 73.

[5] Dwek, E. 1986. *Astrophysical Journal*. **302**: 363.

[6] Henning, Th., Pfau, W. and Altenhoff, W.J. 1990. *Journal Astronomy & Astrophysics*. **227**: 542.

[7] Hildebrand, R.H. 1983. Quat. *Journ. Royal. Astron. Soc*. **24**: 267.

[8] Holmberg, E. 1946. *Medd. Lund Astron. Obs. Ser.* **VI**(117): 1.

[9] Kauch, W. 2002. *M.Sc. (Astronomy) Dissertation*, Innsbruck University, Innsbruck, Austria.

[10] Mebold, U. et al. 1985. *Journal Monthly Notice of Royal Astronomical Society*. **151**: 427.

[11] Mishra, A. 2006. *M.Sc. (Physics) Dissertation*. Tribhuvan University, Kirtipur, Nepal.

[12] Odenwald, S.F. 1988. *Astrophysical Journal*. **325**: 320.

[13] Puget, J.L., Leger, A. and Boulanger, F. 1985. *Journal Astronomy & Astrophysics*. **142**: L19.

[14] Weiland, J. et al. 1986. *Astrophysical Journal*. **306**: L101.

[15] Weinberger, R. and Armsdorfer, B. 2004. *Journal Astronomy & Astrophysics Letters*. **344**: 1.

❐